Eur. Phys. J. C 36, 233–243 (2004)
Digital Object Identifier (DOI) 10.1140/epjc/s2004-01893-2

THE EUROPEAN PHYSICAL JOURNAL C

CP-sensitive observables in $e^+e^- \to \tilde{\chi}_i^0\tilde{\chi}_j^0$ and neutralino decay into the Z boson

A. Bartl[1,a] H. Fraas[2,b], O. Kittel[2,3,c], W. Majerotto[4,d]

[1] Institut für Theoretische Physik, Universität Wien, Boltzmanngasse 5, 1090 Wien, Austria
[2] Institut für Theoretische Physik, Universität Würzburg, Am Hubland, 97074 Würzburg, Germany
[3] Institut de Física Corpuscular – C.S.I.C., Universitat de València Edifici Instituts d'Investigació, Apartat de Correus 22085, 46071 València, Spain
[4] Institut für Hochenergiephysik, Österreichische Akademie der Wissenschaften, Nikolsdorfergasse 18, 1050 Wien, Austria

Received: 4 February 2004 / Revised version: 17 May 2004 /
Published online: 2 July 2004 –

Abstract. We study CP-sensitive observables in the neutralino production $e^+e^- \to \tilde{\chi}_i^0\tilde{\chi}_j^0$ and the subsequent two-body decays of the neutralino $\tilde{\chi}_i^0 \to \chi_n^0 Z$ and of the Z boson $Z \to \ell\bar{\ell}(q\bar{q})$. We identify the CP-odd elements of the Z boson density matrix and propose CP-sensitive triple-product asymmetries. We calculate these observables and the cross sections in the minimal supersymmetric standard model with complex parameters μ and M_1 for an e^+e^- linear collider with $\sqrt{s} = 800\,\mathrm{GeV}$ and longitudinally polarized beams. We show that the asymmetries can reach 3% for $Z \to \ell\bar{\ell}$ and 18% for $Z \to q\bar{q}$ and discuss the feasibility of measuring these asymmetries.

1 Introduction

In the minimal supersymmetric standard model (MSSM) [1] several supersymmetric (SUSY) parameters can be complex. In the neutralino sector of the MSSM these are the $U(1)$ gaugino mass parameter M_1 and the Higgsino mass parameter μ. (The $SU(2)$ gaugino mass parameter M_2 can be made real by redefining the fields.) The physical phases φ_{M_1} and φ_μ of M_1 and μ, respectively, imply CP-odd observables which can in principle be large, because they are already present at tree level. It has been shown that in the production of two different neutralinos $e^+e^- \to \tilde{\chi}_i^0\tilde{\chi}_j^0$ the CP-violating phases cause a non-vanishing neutralino polarization perpendicular to the production plane [2–5], which leads to CP-odd triple-product asymmetries [6] of the neutralino decay products [4, 5, 7–9].

In this work we study CP-violation in neutralino production

$$e^+ + e^- \to \tilde{\chi}_i^0 + \tilde{\chi}_j^0, \quad i,j = 1,\ldots,4, \tag{1}$$

with the subsequent two-body decay of one neutralino into the Z boson (for recent studies see [9, 10])

$$\tilde{\chi}_i^0 \to \chi_n^0 + Z; \quad n < i, \tag{2}$$

and the decay of the Z boson

$$Z \to f + \bar{f}, \quad f = \ell, q, \quad \ell = e,\mu,\tau, \quad q = c, b. \tag{3}$$

In case of CP-violation the non-vanishing phases φ_{M_1} and φ_μ lead to CP-sensitive elements of the Z boson density matrix, which we will discuss in detail. Moreover, these CP-sensitive elements cause CP-odd asymmetries $\mathcal{A}_f$ in the decay distribution of the decay fermions [4],

$$\mathcal{A}_f = \frac{\sigma(\mathcal{T}_f > 0) - \sigma(\mathcal{T}_f < 0)}{\sigma(\mathcal{T}_f > 0) + \sigma(\mathcal{T}_f < 0)}, \tag{4}$$

with σ the cross section and the triple product

$$\mathcal{T}_f = \mathbf{p}_{e^-} \cdot (\mathbf{p}_f \times \mathbf{p}_{\bar{f}}). \tag{5}$$

Due to the correlations between the $\tilde{\chi}_i^0$ polarization and the Z boson polarization, there are CP-odd contributions to the Z boson density matrix and to the asymmetries from the production (1) and from the decay process (2).

The triple product $\mathcal{T}_f$, (5), changes sign under time reversal and is thus T-odd. Due to CPT-invariance, the corresponding T-odd asymmetries $\mathcal{A}_f$ are also CP-odd if final state interactions are neglected. The final state interactions would also contribute to $\mathcal{A}_f$. However, they only arise at loop level and are neglected in the present work.

In Sect. 2 we give our definitions and the formalism used and define the Z boson density matrix. In Sect. 3 we discuss some general properties of the asymmetries. We present numerical results in Sect. 4. Section 5 gives a summary and conclusions.

[a] e-mail: bartl@ap.univie.ac.at
[b] e-mail: fraas@physik.uni-wuerzburg.de
[c] e-mail: kittel@physik.uni-wuerzburg.de
[d] e-mail: majer@qhepu3.oeaw.ac.at

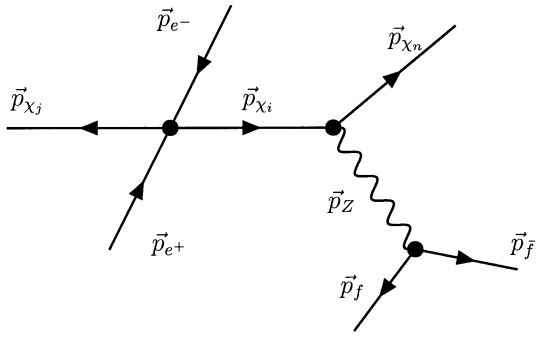

Fig. 1. Schematic picture of the neutralino production and decay process

2 Definitions and formalism

We give the analytic formulae for the differential cross section of the neutralino production

$$e^+ + e^- \to \tilde{\chi}^0_i(p_{\chi_i}, \lambda_i) + \tilde{\chi}^0_j(p_{\chi_j}, \lambda_j), \tag{6}$$

with longitudinally polarized beams and the subsequent decay chain of one of the neutralinos

$$\tilde{\chi}^0_i \to \tilde{\chi}^0_n(p_{\chi_n}, \lambda_n) + Z(p_Z, \lambda_k), \tag{7}$$

$$Z \to f(p_f, \lambda_f) + \bar{f}(p_{\bar{f}}, \lambda_{\bar{f}}). \tag{8}$$

In (6), and (7) and (8), p and λ denote momentum and helicity, respectively. For a schematic picture of the neutralino production and decay process see Fig. 1. In the following we will derive the Z boson spin-density matrix and relate it to the CP-asymmetry $\mathcal{A}_f$ in (4).

2.1 Lagrangian and helicity amplitudes

The interaction Lagrangians relevant for our study are (in our notation and conventions we follow closely [1, 9])

$$\mathcal{L}_{Z^0\tilde{\chi}^0_i\tilde{\chi}^0_j} = \tfrac{1}{2} Z_\mu \bar{\tilde{\chi}}^0_i \gamma^\mu \left[O''^L_{ij} P_L + O''^R_{ij} P_R \right] \tilde{\chi}^0_j, \quad i,j = 1,\ldots,4, \tag{9}$$

$$\mathcal{L}_{e\tilde{e}\tilde{\chi}^0_i} = g f^L_{ei} \bar{e} P_R \tilde{\chi}^0_i \tilde{e}_L + g f^R_{ei} \bar{e} P_L \tilde{\chi}^0_i \tilde{e}_R + \text{h.c.}, \tag{10}$$

$$\mathcal{L}_{Z^0 f\bar{f}} = Z_\mu \bar{f} \gamma^\mu [L_f P_L + R_f P_R] f, \tag{11}$$

with $P_{L,R} = \frac{1}{2}(1 \mp \gamma_5)$. In the neutralino basis $\tilde{\gamma}, \tilde{Z}, \tilde{H}^0_a, \tilde{H}^0_b$ the couplings are

$$O''^L_{ij} = -\frac{1}{2}\frac{g}{\cos\theta_\mathrm{W}} \times \left[(N_{i3}N^*_{j3} - N_{i4}N^*_{j4}) \cos 2\beta + (N_{i3}N^*_{j4} + N_{i4}N^*_{j3}) \sin 2\beta \right], \tag{12}$$

$$O''^R_{ij} = -O''^{L*}_{ij}, \quad L_f = -\frac{g}{\cos\theta_\mathrm{W}}(T_{3f} - q_f \sin^2\theta_\mathrm{W}),$$

$$R_f = \frac{g}{\cos\theta_\mathrm{W}} q_f \sin^2\theta_\mathrm{W}, \tag{13}$$

$$f^L_{\ell i} = -\sqrt{2} \times \left[\frac{1}{\cos\theta_\mathrm{W}} (T_{3\ell} - q_\ell \sin^2\theta_\mathrm{W}) N_{i2} + q_\ell \sin\theta_\mathrm{W} N_{i1} \right], \tag{14}$$

$$f^R_{\ell i} = -\sqrt{2} q_\ell \sin\theta_\mathrm{W} \left[\tan\theta_\mathrm{W} N^*_{i2} - N^*_{i1} \right], \tag{15}$$

with g the weak coupling constant ($g = e/\sin\theta_\mathrm{W}$, $e > 0$), q_f and T_{3f} the charge and the isospin of the fermion, and $\tan\beta = v_2/v_1$ the ratio of the vacuum expectation values of the two neutral Higgs fields. N_{ij} is the complex unitary 4×4 matrix which diagonalizes the neutral gaugino–Higgsino mass matrix $Y_{\alpha\beta}$, $N^*_{i\alpha} Y_{\alpha\beta} N^\dagger_{\beta k} = m_{\tilde{\chi}^0_i}\delta_{ik}$, with $m_{\tilde{\chi}^0_i} > 0$. Note that our definitions of $O''^{L,R}_{ij}$ and L_f, R_f differ from those given in [1, 3] by a factor of $g/\cos\theta_\mathrm{W}$.

The helicity amplitudes $T_P^{\lambda_i\lambda_j}$ for the production process are given in [3]. Those for the two-body decays, (7) and (8), are

$$T^{\lambda_n\lambda_k}_{D_1,\lambda_i} = \bar{u}(p_{\chi_n}, \lambda_n)\gamma^\mu \left[O''^L_{ni} P_L + O''^R_{ni} P_R \right] u(p_{\chi_i}, \lambda_i) \varepsilon^{\lambda_k *}_\mu \tag{16}$$

and

$$T^{\lambda_f\lambda_{\bar{f}}}_{D_2,\lambda_k} = \bar{u}(p_f, \lambda_f)\gamma^\mu [L_f P_L + R_f P_R] v(p_{\bar{f}}, \lambda_{\bar{f}}) \varepsilon^{\lambda_k}_\mu. \tag{17}$$

The polarization vectors $\varepsilon^{\lambda_k}_\mu, \lambda_k = 0, \pm1$, are given in Appendix A. The amplitude for the whole process (6), (7) and (8) is

$$T = \Delta(\tilde{\chi}^0_i)\Delta(Z) \sum_{\lambda_i,\lambda_k} T_P^{\lambda_i\lambda_j} T^{\lambda_n\lambda_k}_{D_1,\lambda_i} T^{\lambda_f\lambda_{\bar{f}}}_{D_2,\lambda_k}, \tag{18}$$

with the neutralino propagator $\Delta(\tilde{\chi}^0_i) = \mathrm{i}/[p^2_{\chi_i} - m^2_{\chi_i} + \mathrm{i} m_{\chi_i}\Gamma_{\chi_i}]$ and the Z boson propagator $\Delta(Z) = \mathrm{i}/[p^2_Z - m^2_Z + \mathrm{i} m_Z \Gamma_Z]$ (the mass and width are denoted by m and Γ, respectively). For these propagators we use the narrow width approximation.

2.2 Cross section and Z boson density matrix

For the calculation of the cross section for the combined process of the neutralino production (6) and the subsequent two-body decays (7) and (8) of $\tilde{\chi}^0_i$ we use the same spin-density matrix formalism as in [3, 11]. The (unnormalized) spin-density matrix of the Z boson,

$$\rho_P(Z)^{\lambda_k\lambda'_k} = |\Delta(\tilde{\chi}^0_i)|^2 \sum_{\lambda_i,\lambda'_i} \rho_P(\tilde{\chi}^0_i)^{\lambda_i\lambda'_i} \rho_{D1}(\tilde{\chi}^0_i)^{\lambda_k\lambda'_k}_{\lambda'_i\lambda_i}, \tag{19}$$

is composed of the spin-density production matrix

$$\rho_P(\tilde{\chi}^0_i)^{\lambda_i\lambda'_i} = \sum_{\lambda_j} T_P^{\lambda_i\lambda_j} T_P^{\lambda'_i\lambda_j\,*} \tag{20}$$

and the decay matrix

$$\rho_{D1}(\tilde{\chi}^0_i)^{\lambda_k\lambda'_k}_{\lambda'_i\lambda_i} = \sum_{\lambda_n} T^{\lambda_n\lambda_k}_{D_1,\lambda_i} T^{\lambda_n\lambda'_k *}_{D_1,\lambda'_i}. \tag{21}$$

With the decay matrix for the Z decay,

$$\rho_{D2}(Z)_{\lambda'_k\lambda_k} = \sum_{\lambda_f,\lambda_{\bar{f}}} T^{\lambda_f\lambda_{\bar{f}}}_{D_2,\lambda_k} T^{\lambda_f\lambda_{\bar{f}}*}_{D_2,\lambda'_k}, \tag{22}$$

the amplitude squared for the complete process $e^+e^- \to \tilde{\chi}^0_i\tilde{\chi}^0_j$; $\tilde{\chi}^0_i \to \tilde{\chi}^0_n Z$; $Z \to f\bar{f}$ can now be written

$$|T|^2 = |\Delta(Z)|^2 \sum_{\lambda_k,\lambda'_k} \rho_P(Z)^{\lambda_k\lambda'_k}\, \rho_{D2}(Z)_{\lambda'_k\lambda_k}. \tag{23}$$

The differential cross section in the laboratory system is then given by

$$\mathrm{d}\sigma = \frac{1}{2s}|T|^2 \mathrm{dLips}(s, p_{\chi_j}, p_{\chi_n}, p_f, p_{\bar{f}}), \tag{24}$$

where $\mathrm{dLips}(s, p_{\chi_j}, p_{\chi_n}, p_f, p_{\bar{f}})$ is the Lorentz invariant phase space element defined in (B.1) of Appendix B. More details concerning kinematics and phase space can be found in Appendices A and B.

For the polarization of the decaying neutralino $\tilde{\chi}^0_i$ with momentum p_{χ_i} we introduce three space-like spin vectors $s^a_{\chi_i}$ $(a = 1,2,3)$, which together with $p^\mu_{\chi_i}/m_{\chi_i}$ form an orthonormal set with $s^a_{\chi_i}\cdot s^b_{\chi_i} = -\delta^{ab}$, $s^a_{\chi_i}\cdot p_{\chi_i} = 0$, then the (unnormalized) neutralino density matrix can be expanded in terms of the Pauli matrices:

$$\rho_P\left(\tilde{\chi}^0_i\right)^{\lambda_i\lambda'_i} = 2\left(\delta_{\lambda_i\lambda'_i} P + \sigma^a_{\lambda_i\lambda'_i}\Sigma^a_P\right), \tag{25}$$

where we sum over a. With our choice of the spin vectors $s^a_{\chi_i}$, given in Appendix A, $\frac{\Sigma^3_P}{P}$ is the longitudinal polarization of the neutralino $\tilde{\chi}^0_i$, $\frac{\Sigma^1_P}{P}$ is the transverse polarization in the production plane and $\frac{\Sigma^2_P}{P}$ is the polarization perpendicular to the production plane. The analytical formulae for P and Σ^a_P are given in [3]. To describe the polarization states of the Z boson, we introduce a set of spin vectors t^c_Z $(c = 1,2,3)$ and choose polarization vectors $\varepsilon^{\lambda_k}_\mu$ $(\lambda_k = 0, \pm 1)$, given in Appendix A. Then we obtain for the decay matrices

$$\rho_{D1}\left(\tilde{\chi}^0_i\right)^{\lambda_k\lambda'_k}_{\lambda'_i\lambda_i} = \left(\delta_{\lambda'_i\lambda_i} D_1^{\mu\nu} + \sigma^a_{\lambda'_i\lambda_i}\Sigma^{a\ \mu\nu}_{D1}\right)\varepsilon^{\lambda_k *}_\mu \varepsilon^{\lambda'_k}_\nu \tag{26}$$

and

$$\rho_{D2}(Z)_{\lambda'_k\lambda_k} = D_2^{\mu\nu}\varepsilon^{\lambda_k}_\mu \varepsilon^{\lambda'_k *}_\nu, \tag{27}$$

with [9]

$$\begin{aligned} D_1^{\mu\nu} = 2\big[&2p^\mu_{\chi_i}p^\nu_{\chi_i} - \left(p^\mu_{\chi_i}p^\nu_Z + p^\nu_{\chi_i}p^\mu_Z\right) \\ &-\tfrac{1}{2}\left(m^2_{\chi_i} + m^2_{\chi_n} - m^2_Z\right) g^{\mu\nu}\big] |O''^L_{ni}|^2 \\ &-2g^{\mu\nu} m_{\chi_i} m_{\chi_n}\left[\left(\mathrm{Re}O''^L_{ni}\right)^2 - \left(\mathrm{Im}O''^L_{ni}\right)^2\right], \end{aligned} \tag{28}$$

$$\begin{aligned} \Sigma^{a\ \mu\nu}_{D_1} = 2\mathrm{i}\Big\{ &- m_{\chi_i}\epsilon^{\mu\alpha\nu\beta} s^a_{\chi_i\alpha}\left(p_{\chi_i\beta} - p_{Z\beta}\right)|O''^L_{ni}|^2 \\ &+2m_{\chi_n}\left(s^{a\mu}_{\chi_i}p^\nu_{\chi_i} - s^{a\nu}_{\chi_i}p^\mu_{\chi_i}\right)\left(\mathrm{Im}O''^L_{ni}\right)\left(\mathrm{Re}O''^L_{ni}\right) \\ &- m_{\chi_n}\epsilon^{\mu\alpha\nu\beta} s^a_{\chi_i\alpha} p_{\chi_i\beta}\left[\left(\mathrm{Re}O''^L_{ni}\right)^2 - \left(\mathrm{Im}O''^L_{ni}\right)^2\right]\Big\} \\ &(\epsilon_{0123} = 1), \end{aligned} \tag{29}$$

and

$$\begin{aligned} D_2^{\mu\nu} = &2\Big(-2p^\mu_{\bar{f}}p^\nu_{\bar{f}} + p^\mu_Z p^\nu_{\bar{f}} + p^\mu_{\bar{f}}p^\nu_Z - \tfrac{1}{2}m^2_Z g^{\mu\nu}\Big)\left(L^2_f + R^2_f\right) \\ &- 2\mathrm{i}\epsilon^{\mu\alpha\nu\beta} p_{Z\alpha} p_{\bar{f}\beta}\left(L^2_f - R^2_f\right). \end{aligned} \tag{30}$$

Due to the Majorana properties of the neutralinos, $D_1^{\mu\nu}$ is symmetric and $\Sigma^{a\ \mu\nu}_{D1}$ is antisymmetric under interchange of μ and ν. In (26) and (27) we use the expansion [12]

$$\begin{aligned} \varepsilon^{\lambda_k}_\mu \varepsilon^{\lambda'_k *}_\nu = &\tfrac{1}{3}\delta^{\lambda'_k\lambda_k} I_{\mu\nu} - \frac{\mathrm{i}}{2m_Z}\epsilon_{\mu\nu\rho\sigma} p^\rho_Z t^{c\sigma}_Z \left(J^c\right)^{\lambda'_k\lambda_k} \\ &-\tfrac{1}{2} t^c_{Z\mu} t^d_{Z\nu}\left(J^{cd}\right)^{\lambda'_k\lambda_k} \quad (\epsilon_{0123} = 1), \end{aligned} \tag{31}$$

summed over c, d. Here, J^c are the 3×3 spin 1 matrices with $[J^c, J^d] = \mathrm{i}\epsilon_{cde}J^e$ and

$$J^{cd} = J^c J^d + J^d J^c - \tfrac{4}{3}\delta^{cd}, \tag{32}$$

with $J^{11} + J^{22} + J^{33} = 0$, are the components of the symmetric, traceless tensor, given in Appendix C, and

$$I_{\mu\nu} = -g_{\mu\nu} + \frac{p_{Z\mu}p_{Z\nu}}{m^2_Z} \tag{33}$$

guarantees the completeness relation of the polarization vectors

$$\sum_{\lambda_k} \varepsilon^{\lambda_k *}_\mu \varepsilon^{\lambda_k}_\nu = -g_{\mu\nu} + \frac{p_{Z\mu}p_{Z\nu}}{m^2_Z}. \tag{34}$$

The second term in (31) describes the vector polarization and the third term describes the tensor polarization of the spin 1 Z boson. The decay matrices can be expanded in terms of the spin matrices J^c and J^{cd}. The first term of the decay matrix ρ_{D1}, (26), which is independent of the neutralino polarization, then gives

$$\begin{aligned} D_1^{\mu\nu}\varepsilon^{\lambda_k *}_\mu \varepsilon^{\lambda'_k}_\nu = &D_1\delta^{\lambda_k\lambda'_k} + {}^c D_1\left(J^c\right)^{\lambda_k\lambda'_k} \\ &+ {}^{cd}D_1\left(J^{cd}\right)^{\lambda_k\lambda'_k}, \end{aligned} \tag{35}$$

summed over c, d, with

$$\begin{aligned} D_1 = &\left[m^2_{\chi_n} - \tfrac{1}{3}m^2_{\chi_i} - m^2_Z + \frac{4}{3}\frac{\left(p_{\chi_i}\cdot p_Z\right)^2}{m^2_Z}\right]|O''^L_{ni}|^2 \\ &+2m_{\chi_i}m_{\chi_n}\left[\left(\mathrm{Re}O''^L_{ni}\right)^2 - \left(\mathrm{Im}O''^L_{ni}\right)^2\right], \end{aligned} \tag{36}$$

$$^{cd}D_1 = -\big[2\left(t^c_Z\cdot p_{\chi_i}\right)\left(t^d_Z\cdot p_{\chi_i}\right)$$

$$+\tfrac{1}{2}\left(m_{\chi_i}^2+m_{\chi_n}^2-m_Z^2\right)\delta^{cd}\big]\,|O_{ni}^{''L}|^2$$
$$-\delta^{cd}m_{\chi_i}m_{\chi_n}\left[\left(\mathrm{Re}O_{ni}^{''L}\right)^2-\left(\mathrm{Im}O_{ni}^{''L}\right)^2\right], \quad (37)$$

and ${}^cD_1=0$ due to the Majorana character of the neutralinos. As a consequence of the completeness relation, (34), the diagonal coefficients are linearly dependent

$${}^{11}D_1+{}^{22}D_1+{}^{33}D_1=-\tfrac{3}{2}D_1. \quad (38)$$

For large three-momentum p_{χ_i}, the Z boson will mainly be emitted into the forward direction with respect to p_{χ_i}, i.e. $\hat{p}_{\chi_i}\approx\hat{p}_Z$, with $\hat{p}=\mathbf{p}/|\mathbf{p}|$, so that $(t_Z^{1,2}\cdot p_{\chi_i})\approx 0$ in (37). Therefore, for high energies ${}^{11}D_1\approx{}^{22}D_1$, and the contributions for the non-diagonal coefficients ${}^{cd}D_1(c\neq d)$ will be small.

For the second term of ρ_{D1}, (26), which depends on the polarization of the decaying neutralino, we obtain

$$\Sigma_{D1}^{a\ \mu\nu}\varepsilon_\mu^{\lambda_k *}\varepsilon_\nu^{\lambda_k'} \quad (39)$$
$$=\Sigma_{D1}^a\delta^{\lambda_k\lambda_k'}+{}^c\Sigma_{D1}^a\left(J^c\right)^{\lambda_k\lambda_k'}+{}^{cd}\Sigma_{D1}^a\left(J^{cd}\right)^{\lambda_k\lambda_k'},$$

summed over c, d, with

$$\begin{aligned}&{}^c\Sigma_{D1}^a\\&=\frac{2}{m_Z}\left\{\left[\left|O_{ni}^{''L}\right|^2 m_{\chi_i}+\left[\left(\mathrm{Re}O_{ni}^{''L}\right)^2-\left(\mathrm{Im}O_{ni}^{''L}\right)^2\right]m_{\chi_n}\right]\right.\\&\quad\times\left[\left(s_{\chi_i}^a\cdot p_Z\right)\left(t_Z^c\cdot p_{\chi_i}\right)-\left(s_{\chi_i}^a\cdot t_Z^c\right)\left(p_Z\cdot p_{\chi_i}\right)\right]\\&\quad+\left|O_{ni}^{''L}\right|^2 m_{\chi_i}m_Z^2\left(s_{\chi_i}^a\cdot t_Z^c\right) \quad (40)\\&\quad\left.-2\left(\mathrm{Im}O_{ni}^{''L}\right)\left(\mathrm{Re}O_{ni}^{''L}\right)m_{\chi_n}\epsilon_{\mu\nu\rho\sigma}s_{\chi_i}^{a\mu}p_{\chi_i}^\nu p_Z^\rho t_Z^{c\sigma}\right\},\end{aligned}$$

and $\Sigma_{D1}^a={}^{cd}\Sigma_{D1}^a=0$ due to the Majorana character of the neutralinos. A similar expansion for the Z decay matrix, (27), results in

$$\rho_{D2}\left(Z\right)_{\lambda_k'\lambda_k}=D_2\delta^{\lambda_k'\lambda_k}+{}^cD_2\left(J^c\right)^{\lambda_k'\lambda_k}+{}^{cd}D_2\left(J^{cd}\right)^{\lambda_k'\lambda_k}, \quad (41)$$

where we sum over c, d, with

$$D_2=\tfrac{2}{3}\left(R_f^2+L_f^2\right)m_Z^2, \quad (42)$$
$${}^cD_2=2\left(R_f^2-L_f^2\right)m_Z\left(t_Z^c\cdot p_{\bar{f}}\right), \quad (43)$$
$${}^{cd}D_2=\left(R_f^2+L_f^2\right)\left[2\left(t_Z^c\cdot p_{\bar{f}}\right)\left(t_Z^d\cdot p_{\bar{f}}\right)-\tfrac{1}{2}m_Z^2\delta^{cd}\right]. \quad (44)$$

As a consequence of the completeness relation, (34), the diagonal coefficients are linearly dependent

$${}^{11}D_2+{}^{22}D_2+{}^{33}D_2=-\tfrac{3}{2}D_2. \quad (45)$$

For large three-momentum p_Z, the fermion $\bar{f}$ will mainly be emitted into the forward direction with respect to p_Z, i.e. $\hat{p}_Z\approx\hat{p}_{\bar{f}}$, so that $(t_Z^{1,2}\cdot p_{\bar{f}})\approx 0$ in (44). Therefore, for high energies ${}^{11}D_2\approx{}^{22}D_2$, and the contributions for the non-diagonal coefficients ${}^{cd}D_2(c\neq d)$ will be small.

Inserting the density matrices (25) and (26) into (19) leads to

$$\rho_P\left(Z\right)^{\lambda_k\lambda_k'}=4\,|\Delta\left(\tilde{\chi}_i^0\right)|^2 \quad (46)$$
$$\times\left[PD_1\delta^{\lambda_k\lambda_k'}+\Sigma_P^a{}^c\Sigma_{D1}^a\left(J^c\right)^{\lambda_k\lambda_k'}+P^{cd}D_1\left(J^{cd}\right)^{\lambda_k\lambda_k'}\right],$$

summed over a, c, d. Inserting then (46) and (27) into (23) leads to

$$\begin{aligned}|T|^2&=4\,|\Delta\left(\tilde{\chi}_i^0\right)|^2\,|\Delta\left(Z\right)|^2\\&\quad\times\left[3PD_1D_2+2\Sigma_P^a{}^c\Sigma_{D1}^a{}^cD_2\right.\\&\qquad\left.+4P\left({}^{cd}D_1^{cd}D_2-\tfrac{1}{3}{}^{cc}D_1{}^{dd}D_2\right)\right], \quad (47)\end{aligned}$$

summed over a, c, d, which is the decomposition of the amplitude squared in its scalar (first term), vector (second term) and tensor part (third term).

2.3 Z boson density matrix

The polarization of the Z boson, produced in the neutralino decay (7), is given by its 3×3 density matrix $\langle\rho(Z)\rangle$ with $\mathrm{Tr}\{\langle\rho(Z)\rangle\}=1$. We obtain $\langle\rho(Z)\rangle$ in the laboratory system by integrating (46) over the Lorentz invariant phase space element

$$\begin{aligned}&\mathrm{dLips}\left(s,p_{\chi_j},p_{\chi_n},p_Z\right)\\&=\frac{1}{(2\pi)^2}\,\mathrm{dLips}(s,p_{\chi_i},p_{\chi_j})\,\mathrm{d}s_{\chi_i}\sum_{\pm}\mathrm{dLips}\left(s_{\chi_i},p_{\chi_n},p_Z^{\pm}\right),\end{aligned}$$

see (B.1), and normalizing by the trace:

$$\begin{aligned}\langle\rho(Z)^{\lambda_k\lambda_k'}\rangle&=\frac{\int\rho_P(Z)^{\lambda_k\lambda_k'}\,\mathrm{dLips}}{\int\mathrm{Tr}\{\rho_P(Z)^{\lambda_k\lambda_k'}\}\,\mathrm{dLips}} \quad (48)\\&=\tfrac{1}{3}\delta^{\lambda_k\lambda_k'}+V_c\,\left(J^c\right)^{\lambda_k\lambda_k'}+T_{cd}\,\left(J^{cd}\right)^{\lambda_k\lambda_k'},\end{aligned}$$

summed over c, d. The vector and tensor coefficients V_c and T_{cd} are given by

$$V_c=\frac{\int|\Delta\left(\tilde{\chi}_i^0\right)|^2\,\Sigma_P^a{}^c\Sigma_{D1}^a\,\mathrm{dLips}}{3\int|\Delta\left(\tilde{\chi}_i^0\right)|^2\,PD_1\,\mathrm{dLips}},$$
$$T_{cd}=T_{dc}=\frac{\int|\Delta\left(\tilde{\chi}_i^0\right)|^2\,P\,{}^{cd}D_1\,\mathrm{dLips}}{3\int|\Delta\left(\tilde{\chi}_i^0\right)|^2\,PD_1\,\mathrm{dLips}}, \quad (49)$$

with sum over a. The tensor coefficients T_{12} and T_{23} vanish due to phase space integration. The density matrix in the circular basis, see (A.11), is given by

$$\langle\rho(Z)^{--}\rangle=\tfrac{1}{2}-V_3+T_{33}, \quad (50)$$
$$\langle\rho(Z)^{00}\rangle=-2T_{33}, \quad (51)$$
$$\langle\rho(Z)^{-0}\rangle=\tfrac{1}{\sqrt{2}}(V_1+\mathrm{i}V_2)-\sqrt{2}\,T_{13}, \quad (52)$$

$$\langle\rho(Z)^{-+}\rangle = T_{11}, \tag{53}$$

$$\langle\rho(Z)^{0+}\rangle = \tfrac{1}{\sqrt{2}}(V_1 + \mathrm{i}V_2) + \sqrt{2}\,T_{13}, \tag{54}$$

where we have used $T_{11}+T_{22}+T_{33} = -\frac{1}{2}$ and $T_{12} = T_{23} = 0$.

3 T-odd asymmetry

From (47) one obtains for the asymmetry, (4):

$$\mathcal{A}_f = \frac{\int \mathrm{Sign}[\mathcal{T}_f]|T|^2 \mathrm{dLips}}{\int |T|^2 \mathrm{dLips}} \tag{55}$$

$$= \frac{\int |\Delta\left(\tilde{\chi}^0_i\right)|^2 |\Delta(Z)|^2\ \mathrm{Sign}[\mathcal{T}_f] 2\Sigma^a_P\, {}^c\Sigma^a_{D1}\, {}^cD_2 \mathrm{dLips}}{\int |\Delta\left(\tilde{\chi}^0_i\right)|^2 |\Delta(Z)|^2\ 3PD_1D_2 \mathrm{dLips}},$$

summed over a, c. In the numerator only the vector part of $|T|^2$ remains because only the vector part contains the triple product[1] $\mathcal{T}_f = \mathbf{p}_{e^-} \cdot (\mathbf{p}_f \times \mathbf{p}_{\bar{f}})$. In the denominator the vector and tensor parts of $|T|^2$ vanish, because for complete phase space integrations the spin correlations are eliminated. Due to the correlations between the $\tilde{\chi}^0_i$ and the Z boson polarization, $\Sigma^a_P\, {}^c\Sigma^a_{D1}$, there are CP-odd contributions to the asymmetry $\mathcal{A}_f$ which stem from the neutralino production process, see (6), and/or from the neutralino decay process, see (7). The contribution from the production is given by the term with $a = 2$ in (55) and it is proportional to Σ^2_P, (25), which is the transverse polarization of the neutralino perpendicular to the production plane. For $e^+e^- \to \tilde{\chi}^0_i\tilde{\chi}^0_i$ we have $\Sigma^2_P = 0$. The contributions from the decay, which are the terms with $a = 1, 3$ in (55), are proportional to

$$\begin{aligned} &{}^c\Sigma^a_{D1}\, {}^cD_2 \supset \\ &-8m_{\chi_n}\left(\mathrm{Im}O''^L_{ni}\right)\left(\mathrm{Re}O''^L_{ni}\right)\left(R^2_f - L^2_f\right)\left(t^c_Z \cdot p_{\bar{f}}\right) \\ &\quad \times \epsilon_{\mu\nu\rho\sigma} s^{a\mu}_{\chi_i} p^\nu_{\chi_i} p^\rho_Z t^{c\sigma}_Z, \end{aligned} \tag{56}$$

see last term of (40), which contains the ϵ-tensor. Thus $\mathcal{A}_f$ can be enhanced (reduced) if the contributions from production and decay have the same (opposite) sign. Note that the contributions from the decay would vanish for a two-body decay of the neutralino into a scalar particle. In this case the remaining contributions from the production are multiplied by a decay factor $\propto (|R|^2 - |L|^2)$ [7], and thus $\mathcal{A}_f \propto (|R|^2 - |L|^2)/(|R|^2 + |L|^2)$, where R and L are the right and left couplings of the scalar particle to the neutralino.

For the measurement of $\mathcal{A}_f$ the charges and the flavors of f and $\bar{f}$ have to be distinguished. For $f = e, \mu$ this will be possible on an event by event basis. For $f = \tau$ it will be possible after taking into account corrections due to the reconstruction of the τ momentum. For $f = q$ the distinction of the quark flavors should be possible by flavor tagging in the case $q = b, c$ [13]. However, in this case the quark charges will be distinguished statistically for a given event sample only [14]. Note that $\mathcal{A}_q$ is always larger than $\mathcal{A}_\ell$, due to the dependence of $\mathcal{A}_f$ on the Z-$\bar{f}$-f couplings [4, 9]:

$$\mathcal{A}_f \propto \frac{R^2_f - L^2_f}{R^2_f + L^2_f} \Rightarrow \tag{57}$$

$$\mathcal{A}_{b(c)} = \frac{R^2_\ell + L^2_\ell}{R^2_\ell - L^2_\ell}\,\frac{R^2_{b(c)} - L^2_{b(c)}}{R^2_{b(c)} + L^2_{b(c)}}\ \mathcal{A}_\ell \simeq 6.3\ (4.5) \times \mathcal{A}_\ell,$$

which follows from (42), (43) and (55).

The relative statistical error of $\mathcal{A}_f$ is given by $\delta\mathcal{A}_f = \Delta\mathcal{A}_f/|\mathcal{A}_f| = S_f/(|\mathcal{A}_f|\sqrt{N})$ [7], with S_f standard deviations and $N = \mathcal{L} \cdot \sigma_t$ the number of events with $\mathcal{L}$ the integrated luminosity and the cross section $\sigma_t = \sigma(e^+e^- \to \tilde{\chi}^0_i\tilde{\chi}^0_j) \times \mathrm{BR}(\tilde{\chi}^0_i \to Z\tilde{\chi}^0_n) \times \mathrm{BR}(Z \to f\bar{f})$. Taking $\delta\mathcal{A}_f = 1$ it follows $S_f = |\mathcal{A}_f|\sqrt{N}$. Note that S_f is larger for $f = b, c$ than for $f = \ell = e, \mu, \tau$ with $S_b \simeq 7.7 \times S_\ell$ and $S_c \simeq 4.9 \times S_\ell$, which follows from (57) and from $\mathrm{BR}(Z \to b\bar{b}) \simeq 1.5 \times \mathrm{BR}(Z \to \ell\bar{\ell})$, $\mathrm{BR}(Z \to c\bar{c}) \simeq 1.2 \times \mathrm{BR}(Z \to \ell\bar{\ell})$.

4 Numerical results

We present numerical results for the Z density matrix $\langle\rho(Z)\rangle$, (49), the asymmetry $\mathcal{A}_\ell (\ell = e, \mu, \tau)$, (4), and the cross section $\sigma_t = \sigma(e^+e^- \to \tilde{\chi}^0_i\tilde{\chi}^0_j) \times \mathrm{BR}(\tilde{\chi}^0_i \to \tilde{\chi}^0_1 Z) \times \mathrm{BR}(Z \to \ell\bar{\ell})$. For the branching ratio $Z \to \ell\bar{\ell}$, summed over $\ell = e, \mu, \tau$, we take the experimental value $\mathrm{BR}(Z \to \ell\bar{\ell}) = 0.1$ [15]. The values for $\mathcal{A}_{b,c}$ may be obtained from (57). We choose a center of mass energy of $\sqrt{s} = 800\,\mathrm{GeV}$ and longitudinally polarized beams with beam polarizations $(P_{e^-}, P_{e^+}) = (\pm 0.8, \mp 0.6)$. We study the dependence of $\langle\rho(Z)\rangle$, $\mathcal{A}_\ell$ and σ_t on the MSSM parameters $\mu = |\mu|\,\mathrm{e}^{\mathrm{i}\,\varphi_\mu}$ and $M_1 = |M_1|\,\mathrm{e}^{\mathrm{i}\,\varphi_{M_1}}$. For all scenarios we keep $\tan\beta = 10$. In order to reduce the number of parameters, we assume the relation $|M_1| = 5/3 M_2 \tan^2\theta_\mathrm{W}$ and use the renormalization group equations [16] for the selectron and smuon masses, $m^2_{\tilde{\ell}_R} = m^2_0 + 0.23 M^2_2 - m^2_Z \cos 2\beta \sin^2\theta_\mathrm{W}$, $m^2_{\tilde{\ell}_L} = m^2_0 + 0.79 M^2_2 + m^2_Z \cos 2\beta(-1/2 + \sin^2\theta_\mathrm{W})$, taking $m_0 = 300\,\mathrm{GeV}$.

Our numerical results presented below are obtained at tree level. One-loop corrections to $e^+e^- \to \tilde{\chi}^0_i\tilde{\chi}^0_j$ have been given in [17] for real MSSM parameters. They are of the order of a few percent and may reach values up to 10%. As the bulk of the one-loop corrections are presumably CP-even, we expect that they will not significantly change our tree-level result for $\mathcal{A}_f$. For an appropriate analysis of the one-loop corrections to $\mathcal{A}_f$ it would be necessary to adopt the formulae of [17] to the case of complex MSSM parameters, which is beyond the scope of the present paper.

The experimental upper limits on the electric dipole moments (EDMs) of electron and neutron may restrict the phases φ_μ and φ_{M_1}. These restrictions are very model dependent. They are less severe when cancellations between

[1] Note that if one would replace the triple product $\mathcal{T}_f$ by $\mathcal{T}_f = \mathbf{p}_{e^-} \cdot (\mathbf{p}_{\chi_i} \times \mathbf{p}_Z)$, and would calculate the corresponding asymmetry, where the Z boson polarization is summed, all spin correlations and thus this asymmetry would vanish identically because of the Majorana properties of the neutralinos.

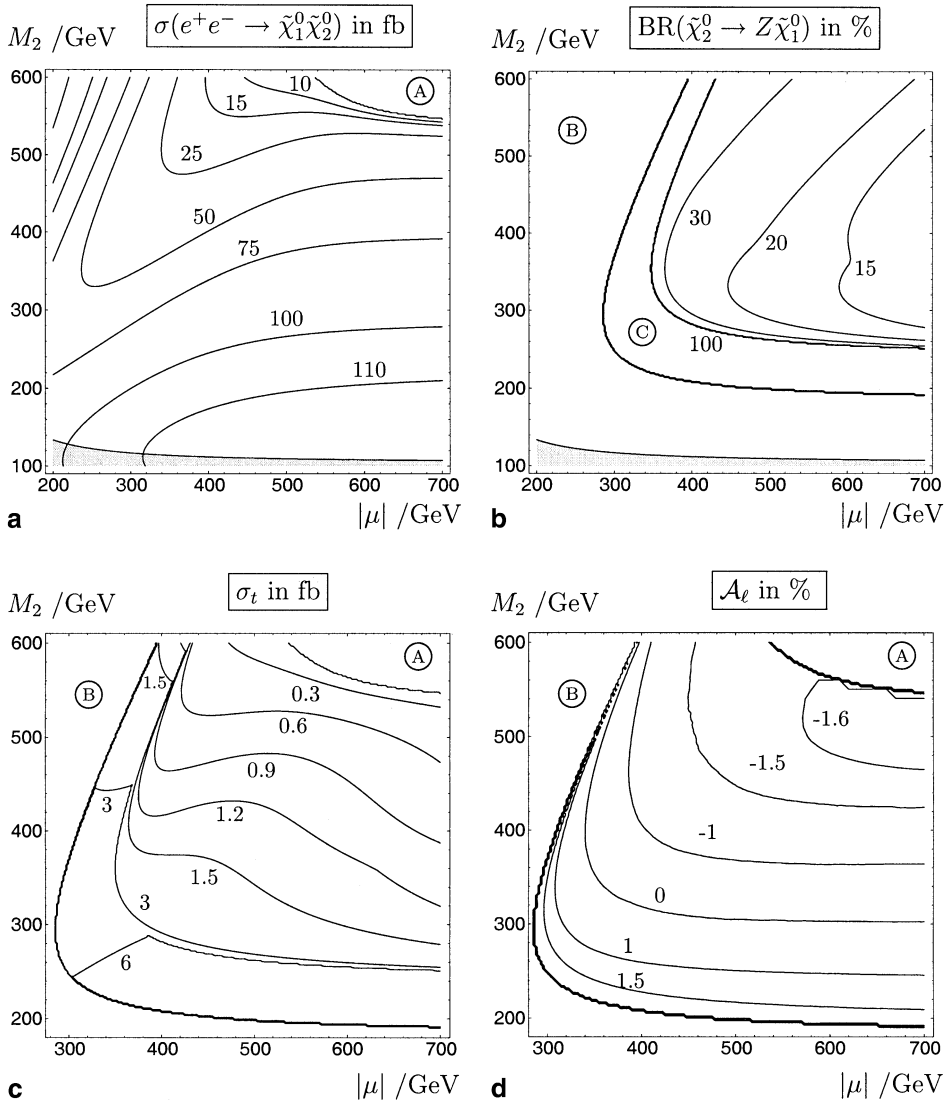

Fig. 2. Contour plots for **a** $\sigma(e^+e^- \to \tilde{\chi}^0_1\tilde{\chi}^0_2)$, **b** BR($\tilde{\chi}^0_2 \to Z\tilde{\chi}^0_1$), **c** $\sigma_t = \sigma(e^+e^- \to \tilde{\chi}^0_1\tilde{\chi}^0_2) \times$ BR($\tilde{\chi}^0_2 \to Z\tilde{\chi}^0_1$) $\times$ BR($Z \to \ell\bar{\ell}$) with BR($Z \to \ell\bar{\ell}$) = 0.1, (2d) the asymmetry $\mathcal{A}_\ell$, in the $|\mu|$–M_2 plane for $\varphi_{M_1} = 0.5\pi$, $\varphi_\mu = 0$, taking $\tan\beta = 10$, $m_0 = 300\,\text{GeV}$, $\sqrt{s} = 800\,\text{GeV}$ and $(P_{e^-}, P_{e^+}) = (-0.8, 0.6)$. The area A (B) is kinematically forbidden by $m_{\tilde{\chi}^0_1} + m_{\tilde{\chi}^0_2} > \sqrt{s}$ ($m_Z + m_{\tilde{\chi}^0_1} > m_{\tilde{\chi}^0_2}$). In area C of plot (2b) BR($\tilde{\chi}^0_2 \to Z\tilde{\chi}^0_1$) = 100%. The gray area is excluded by $m_{\tilde{\chi}^\pm_1} < 104\,\text{GeV}$

the contributions of different SUSY phases occur. For example, in the constrained MSSM the phase φ_μ is restricted to $|\varphi_\mu| \lesssim 0.1\pi$, whereas the phase φ_{M_1} is not restricted, but correlated with φ_μ [18]. In most of our numerical examples below we have chosen $\varphi_{M_1} = \pm\pi/2$, $\varphi_\mu = 0$, which agrees with the constraints from the electron and neutron EDMs. In order to show the full phase dependences of the CP-asymmetry $\mathcal{A}_f$, in one example we study its φ_μ behavior in the whole φ_μ range, relaxing in this case the restrictions from the EDMs. However, as shown in [19], if also lepton flavor violating terms are included, the EDM constraints on φ_μ disappear.

For the calculation of the neutralino widths Γ_{χ_i} and the branching ratios BR($\tilde{\chi}^0_i \to \tilde{\chi}^0_1 Z$) we neglect three-body decays and include the following two-body decays, if kinematically allowed,

$$\tilde{\chi}^0_i \to \tilde{e}_{R,L}e,\ \tilde{\mu}_{R,L}\mu,\ \tilde{\tau}_m\tau,\ \tilde{\nu}_\ell\bar{\nu}_\ell,\ \tilde{\chi}^0_n Z,\ \tilde{\chi}^\mp_m W^\pm,\ \tilde{\chi}^0_n H^0_1,$$
$$\ell = e, \mu, \tau,\ m = 1, 2,\ n < i \qquad (58)$$

with H^0_1 being the lightest neutral Higgs boson. The Higgs parameter is chosen $m_A = 1000\,\text{GeV}$ and thus the decays $\tilde{\chi}^0_i \to \tilde{\chi}^\pm_n H^\mp$ into the charged Higgs bosons, and the decays $\tilde{\chi}^0_i \to \tilde{\chi}^0_n\ H^0_{2,3}$ into the heavy neutral Higgs bosons are forbidden in our scenarios. In the stau sector, we fix the trilinear scalar coupling parameter $A_\tau = 250\,\text{GeV}$.

4.1 Production of $\tilde{\chi}^0_1\,\tilde{\chi}^0_2$

In Fig. 2a we show the cross section for $\tilde{\chi}^0_1\tilde{\chi}^0_2$ production in the $|\mu|$–M_2 plane for $\varphi_\mu = 0$ and $\varphi_{M_1} = 0.5\pi$. For $|\mu| \gtrsim 250\,\text{GeV}$ the left selectron exchange dominates due to the larger $\tilde{\chi}^0_2$–$\tilde{e}_L$ coupling, so that the choice of polarization $(P_{e^-}, P_{e^+}) = (-0.8, 0.6)$ enhances the cross section, which reaches values of more than 110 fb.

The branching ratio BR($\tilde{\chi}^0_2 \to Z\tilde{\chi}^0_1$) is shown in Fig. 2b. The branching ratio can even be 100% and decreases with increasing $|\mu|$ and M_2, when the two-body decays into sleptons and/or into the lightest neutral Higgs boson are kinematically allowed.

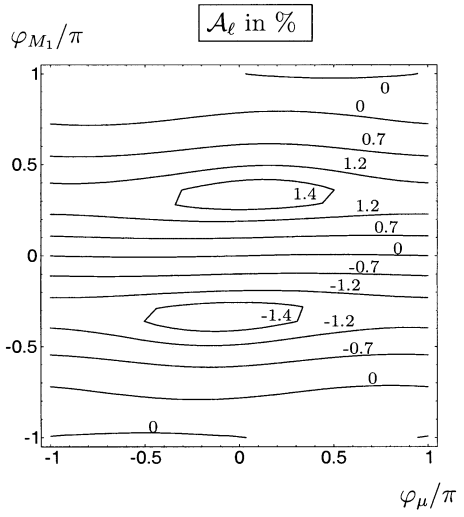

Fig. 3. Contour lines of the asymmetry $\mathcal{A}_\ell$ for $e^+e^- \to \tilde{\chi}^0_1\tilde{\chi}^0_2; \tilde{\chi}^0_2 \to Z\tilde{\chi}^0_1; Z \to \ell\bar{\ell}(\ell = e, \mu, \tau)$, in the φ_μ–φ_{M_1} plane for $M_2 = 250\,\text{GeV}$ and $|\mu| = 400\,\text{GeV}$, taking $\tan\beta = 10$, $m_0 = 300\,\text{GeV}$, $\sqrt{s} = 800\,\text{GeV}$ and $(P_{e^-}, P_{e^+}) = (-0.8, 0.6)$

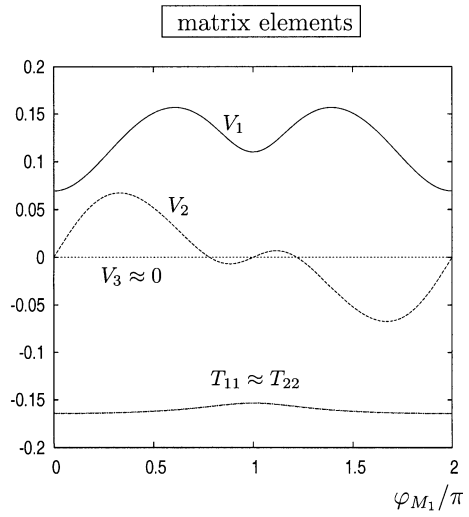

Fig. 4. Dependence on φ_{M_1} of the vector (V_i) and tensor (T_{ii}) elements of the Z density matrix $< \rho(Z) >$, for $e^+e^- \to \tilde{\chi}^0_1\tilde{\chi}^0_2; \tilde{\chi}^0_2 \to Z\tilde{\chi}^0_1$, for $M_2 = 250\,\text{GeV}$ and $|\mu| = 400\,\text{GeV}$, taking $\varphi_\mu = 0$, $\tan\beta = 10$, $m_0 = 300\,\text{GeV}$, $\sqrt{s} = 800\,\text{GeV}$ and $(P_{e^-}, P_{e^+}) = (-0.8, 0.6)$

The cross section $\sigma_t = \sigma(e^+e^- \to \tilde{\chi}^0_1\tilde{\chi}^0_2) \times \text{BR}(\tilde{\chi}^0_2 \to Z\tilde{\chi}^0_1) \times \text{BR}(Z \to \ell\bar{\ell})$ is shown in Fig. 2c. Due to the small branching ratio $\text{BR}(Z \to \ell\bar{\ell}) = 0.1$, σ_t does not exceed 7 fb.

Figure 2d shows the $|\mu|$–M_2 dependence of the asymmetry $\mathcal{A}_\ell$ for $\varphi_{M_1} = 0.5\pi$ and $\varphi_\mu = 0$. The asymmetry $|\mathcal{A}_\ell|$ can reach a value of 1.6%. On contour 0 in Fig. 2d, the (positive) contributions from the production cancel the (negative) contributions from the decay.

We also studied the φ_μ dependence of $\mathcal{A}_\ell$. In the $|\mu|$–M_2 plane for $\varphi_{M_1} = 0$ and $\varphi_\mu = 0.5\pi$ we found $|\mathcal{A}_\ell| < 0.5\%$.

In Fig. 3 we show the φ_μ–φ_{M_1} dependence of $\mathcal{A}_\ell$ for $|\mu| = 400\,\text{GeV}$ and $M_2 = 250\,\text{GeV}$. The value of $\mathcal{A}_\ell$ depends stronger on φ_{M_1} than on φ_μ. It is remarkable that the maximal phases of $\varphi_{M_1}, \varphi_\mu = \pm\pi/2$ do not lead to the highest values of $\mathcal{A}_\ell \approx \pm 1.4\%$, which are reached for $(\varphi_{M_1}, \varphi_\mu) \approx (\pm 0.3\pi, 0)$. The reason for this is that the spin-correlation terms $\Sigma^a_P{}^c\Sigma^a_{D1}{}^cD_2$ in the numerator of $\mathcal{A}_f$, (55), are products of CP-odd and CP-even factors. The CP-odd (CP-even) factors have a sine-like (cosine-like) phase dependence. Therefore, the maximum of the CP-asymmetry $\mathcal{A}_f$ is shifted from $\varphi_{M_1}, \varphi_\mu = \pm\pi/2$ to a smaller or larger value.

In the φ_μ–φ_{M_1} region shown in Fig. 3 also the cross section $\sigma_t = \sigma(e^+e^- \to \tilde{\chi}^0_1\tilde{\chi}^0_2) \times \text{BR}(\tilde{\chi}^0_2 \to Z\tilde{\chi}^0_1) \times \text{BR}(Z \to \ell\bar{\ell})$ with $\text{BR}(\tilde{\chi}^0_2 \to Z\tilde{\chi}^0_1) = 1$ and $\text{BR}(Z \to \ell\bar{\ell}) = 0.1$, is rather insensitive to φ_μ and ranges between 7 fb ($\varphi_{M_1} = 0$) and 14 fb ($\varphi_{M_1} = \pm\pi$).

For the leptonic decay of the Z, the standard deviations are given by $S_\ell = |\mathcal{A}_\ell|\sqrt{\mathcal{L} \cdot \sigma_t}$, and for the hadronic decays by $S_{b(c)} = 7.7(4.9)S_\ell$; see Sect. 3. For $\mathcal{L} = 500\,\text{fb}^{-1}$ and $(\varphi_{M_1}, \varphi_\mu) = (\pm 0.3\pi, 0)$ in Fig. 3 we find $S_{b(c)} = 8(5)$ and thus $\mathcal{A}_{b(c)}$ could be measured. However note that we have $S_\ell < 1$ in this scenario and thus $\mathcal{A}_\ell$ cannot be measured at the 68% confidence level ($S_\ell = 1$).

In Fig. 4 we show the φ_{M_1} dependence of the vector (V_i) and tensor (T_{ii}) elements of the Z density matrix $\langle\rho(Z)\rangle$. The elements T_{11}, T_{22} and V_1 have a CP-even behavior. The element V_2 is CP-odd and is not only zero at $\varphi_{M_1} = 0$ and $\varphi_{M_1} = \pi$, but also at $\varphi_{M_1} \approx (1 \pm 0.2)\pi$, which is due to the destructive interference of the contributions from CP-violation in production and decay. The interference of the contributions from the CP-even effects in production and decay cause the two maxima of V_1. As discussed in Sect. 2.2, the tensor elements T_{11} and T_{22} are almost equal. Compared to V_1 and V_2, they have the same order of magnitude, but their dependence on φ_{M_1} is rather weak. Furthermore, the other elements are small, i.e. $T_{13}, V_3 < 10^{-6}$ and thus the density matrix $\langle\rho(Z)\rangle$ assumes a symmetric shape. In the CP-conserving case, e.g. for $\varphi_{M_1} = \varphi_\mu = 0$, $M_2 = 250\,\text{GeV}$, $|\mu| = 400\,\text{GeV}$, $\tan\beta = 10$, $m_0 = 300\,\text{GeV}$, $\sqrt{s} = 800\,\text{GeV}$ and $(P_{e^-}, P_{e^+}) = (-0.8, 0.6)$ it reads

$$\langle\rho(Z)\rangle = \begin{pmatrix} 0.329 & 0.049 & 0.0003 \\ 0.049 & 0.343 & 0.049 \\ 0.0003 & 0.049 & 0.329 \end{pmatrix}. \tag{59}$$

In the CP-violating case, e.g. for $\varphi_{M_1} = 0.5\pi$ and the other parameters as above, $\langle\rho(Z)\rangle$ has imaginary parts due to a non-vanishing V_2:

$$\langle\rho(Z)\rangle = \tag{60}$$
$$\begin{pmatrix} 0.324 & 0.107 + 0.037\text{i} & 0.0003 \\ 0.107 - 0.037\text{i} & 0.352 & 0.107 + 0.037\text{i} \\ 0.0003 & 0.107 - 0.037\text{i} & 0.324 \end{pmatrix}.$$

Imaginary parts of $\langle\rho(Z)\rangle$ are thus an indication of CP-violation. Note that also the diagonal elements, being CP-even quantities, are changed for $\varphi_{M_1} \neq 0$ and $\varphi_\mu \neq 0$. This fact has been exploited in [10] as a possibility to determine the CP-violating phases.

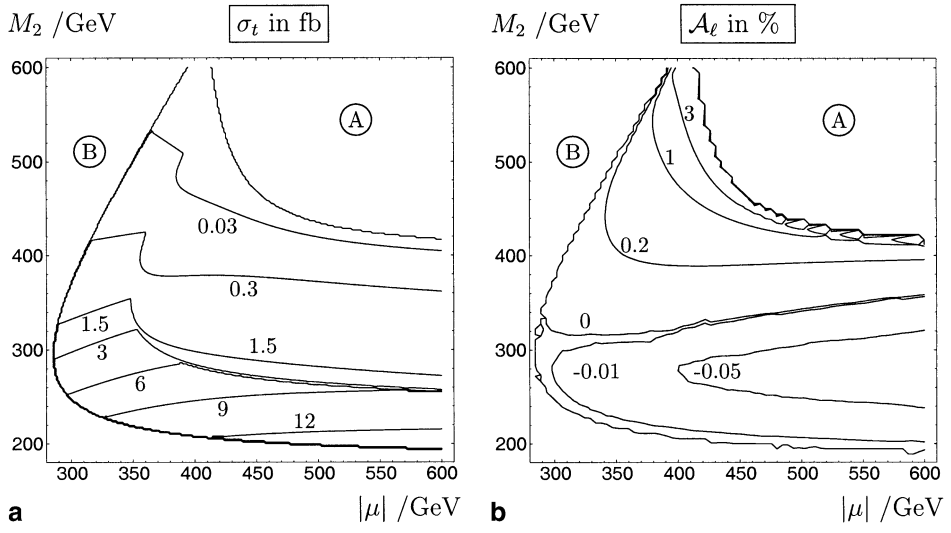

Fig. 5. Contour lines of $\sigma_t = \sigma(e^+e^- \to \tilde{\chi}^0_2\tilde{\chi}^0_2) \times \mathrm{BR}(\tilde{\chi}^0_2 \to Z\tilde{\chi}^0_1) \times \mathrm{BR}(Z \to \ell\bar{\ell})$ **a**, and the asymmetry $\mathcal{A}_\ell$ **b** in the $|\mu|$–M_2 plane for $\varphi_{M_1} = 0.5\pi$, $\varphi_\mu = 0$, taking $\tan\beta = 10$, $m_0 = 300\,\mathrm{GeV}$, $\sqrt{s} = 800\,\mathrm{GeV}$ and $(P_{e^-}, P_{e^+}) = (-0.8, 0.6)$. The area A (B) is kinematically forbidden by $m_{\tilde{\chi}^0_2} + m_{\tilde{\chi}^0_2} > \sqrt{s}$ ($m_Z + m_{\tilde{\chi}^0_1} > m_{\tilde{\chi}^0_2}$)

4.2 Production of $\tilde{\chi}^0_2\,\tilde{\chi}^0_2$

In Fig. 5a we show the cross section $\sigma_t = \sigma(e^+e^- \to \tilde{\chi}^0_2\tilde{\chi}^0_2) \times \mathrm{BR}(\tilde{\chi}^0_2 \to Z\tilde{\chi}^0_1) \times \mathrm{BR}(Z \to \ell\bar{\ell})$ in the $|\mu|$–M_2 plane for $\varphi_\mu = 0$ and $\varphi_{M_1} = 0.5\pi$. The production cross section $\sigma(e^+e^- \to \tilde{\chi}^0_2\tilde{\chi}^0_2)$, which is not shown, is enhanced by the choice $(P_{e^-}, P_{e^+}) = (-0.8, 0.6)$ and reaches values up to 130 fb. The branching ratio $\mathrm{BR}(\tilde{\chi}^0_2 \to Z\tilde{\chi}^0_1)$, shown in Fig. 2b, can be 100%. However, due to the small branching ratio $\mathrm{BR}(Z \to \ell\bar{\ell}) = 0.1$, the cross section shown in Fig. 5a does not exceed 13 fb.

If two equal neutralinos are produced, the CP-sensitive transverse polarization of the neutralinos perpendicular to the production plane vanishes, $\Sigma^2_P = 0$ in (55). However, the asymmetry $\mathcal{A}_f$ need not vanish, because there are CP-sensitive contributions from the neutralino decay process, terms with $a = 1, 3$ in (56). In Fig. 5b we show the $|\mu|$ and M_2 dependence of the asymmetry $\mathcal{A}_\ell$, which reaches more than 3% for $\varphi_{M_1} = 0.5\pi$ and $\varphi_\mu = 0$. Along the zero contour in Fig. 5b the contribution to $\mathcal{A}_\ell$ which is proportional to Σ^1_P, see (55), cancels the one which is proportional to Σ^3_P. As the largest values of $\mathcal{A}_\ell \gtrsim 0.2\%$ and $\mathcal{A}_q \gtrsim 1\%$ lie in a region of the $|\mu|$–M_2 plane where $\sigma_t \lesssim 0.3\,\mathrm{fb}$, it will be difficult to measure $\mathcal{A}_f$ in a statistically significant way. We also studied the φ_μ dependence of $\mathcal{A}_\ell$. In the $|\mu|$–M_2 plane for $\varphi_{M_1} = 0$ and $\varphi_\mu = 0.5\pi$ we found $|\mathcal{A}_\ell| < 0.5\%$, and thus the influence of φ_μ is also small.

In Fig. 6 we show the φ_{M_1} dependence of the vector (V_i) and tensor (T_{ii}) elements of the Z density matrix $\langle\rho(Z)\rangle$. Because there are only CP-sensitive contributions from the neutralino decay process, V_2 is only zero at $\varphi_{M_1} = 0, \pi$ and V_1 has one maximum at $\varphi_{M_1} = \pi$, compared to the elements shown in Fig. 4. In addition, in Fig. 6 the vector elements V_1 and V_2 are much smaller than the tensor elements $T_{11} \approx T_{22}$, compared to Fig. 4. The smallness of the vector element V_2 accounts for the smallness of the asymmetry $|\mathcal{A}_\ell| < 0.05\%$. Furthermore, the other elements are small, i.e. $T_{13} < 10^{-6}$ and $V_3 = 0$.

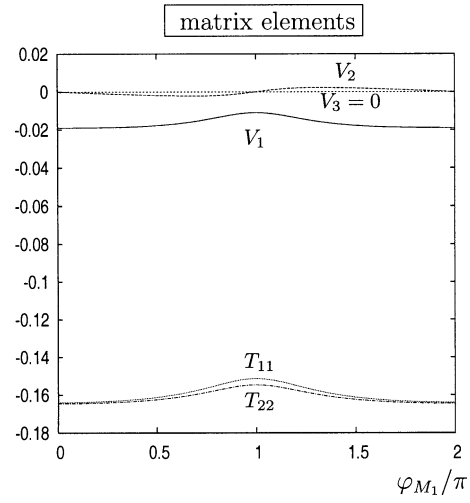

Fig. 6. Dependence on φ_{M_1} of the vector (V_i) and tensor (T_{ii}) elements of the Z density matrix $\langle\rho(Z)\rangle$, for $e^+e^- \to \tilde{\chi}^0_2\tilde{\chi}^0_2; \tilde{\chi}^0_2 \to Z\tilde{\chi}^0_1$, for $M_2 = 250\,\mathrm{GeV}$ and $|\mu| = 400\,\mathrm{GeV}$, taking $\varphi_\mu = 0$, $\tan\beta = 10$, $m_0 = 300\,\mathrm{GeV}$, $\sqrt{s} = 800\,\mathrm{GeV}$ and $(P_{e^-}, P_{e^+}) = (-0.8, 0.6)$

4.3 Production of $\tilde{\chi}^0_1\,\tilde{\chi}^0_3$

In Fig. 7a we show the cross section $\sigma_t = \sigma(e^+e^- \to \tilde{\chi}^0_1\tilde{\chi}^0_3) \times \mathrm{BR}(\tilde{\chi}^0_3 \to Z\tilde{\chi}^0_1) \times \mathrm{BR}(Z \to \ell\bar{\ell})$ in the $|\mu|$–M_2 plane for $\varphi_\mu = 0$ and $\varphi_{M_1} = 0.5\pi$. The production cross section $\sigma(e^+e^- \to \tilde{\chi}^0_1\tilde{\chi}^0_3)$, which is not shown, is enhanced by the choice $(P_{e^-}, P_{e^+}) = (0.8, -0.6)$ and reaches up to 50 fb. The branching ratio $\mathrm{BR}(\tilde{\chi}^0_3 \to Z\tilde{\chi}^0_1)$, which is not shown, can be 1. However, due to the small branching ratio $\mathrm{BR}(Z \to \ell\bar{\ell}) = 0.1$, the cross section shown in Fig. 7a does not exceed 5 fb.

In Fig. 7b we show the $|\mu|$–M_2 dependence of the asymmetry $\mathcal{A}_\ell$. The asymmetry $|\mathcal{A}_\ell|$ reaches 1.3% at its maximum, however in a region, where $\sigma_t < 0.3\,\mathrm{fb}$; the asymmetry $\mathcal{A}_\ell$ thus cannot be measured. We also studied the φ_μ dependence of $\mathcal{A}_\ell$. In the $|\mu|$–M_2 plane for $\varphi_{M_1} = 0$ and $\varphi_\mu = 0.5\pi$ we found $|\mathcal{A}_\ell| < 0.7\%$.

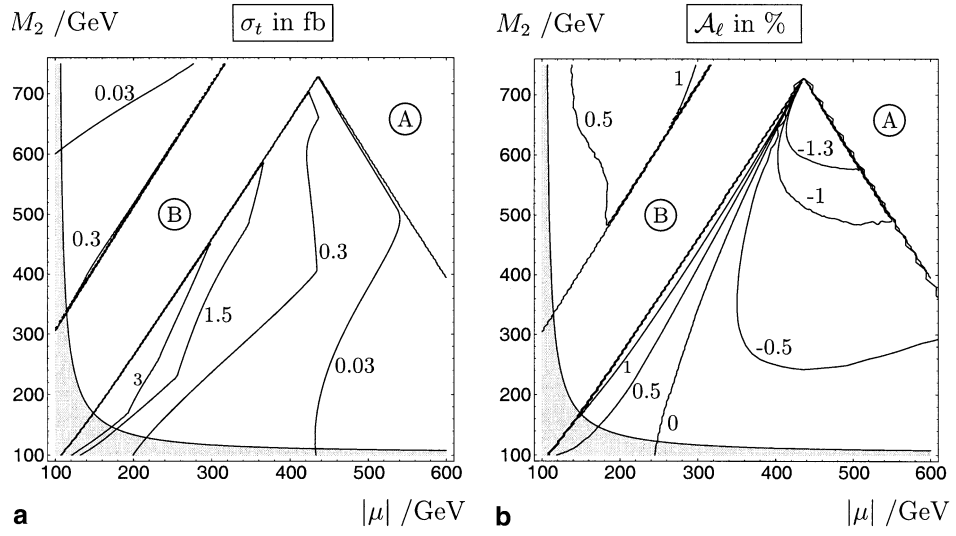

Fig. 7. Contour lines of $\sigma_t = \sigma(e^+e^- \to \tilde{\chi}^0_1\tilde{\chi}^0_3) \times \mathrm{BR}(\tilde{\chi}^0_3 \to Z\tilde{\chi}^0_1) \times \mathrm{BR}(Z \to \ell\bar{\ell})$ **a**, and the asymmetry $\mathcal{A}_\ell$ **b** in the $|\mu|$–M_2 plane for $\varphi_{M_1} = 0.5\pi$, $\varphi_\mu = 0$, taking $\tan\beta = 10$, $m_0 = 300\,\mathrm{GeV}$, $\sqrt{s} = 800\,\mathrm{GeV}$ and $(P_{e^-}, P_{e^+}) = (0.8, -0.6)$. The area A (B) is kinematically forbidden by $m_{\tilde{\chi}^0_1} + m_{\tilde{\chi}^0_3} > \sqrt{s}$ ($m_Z + m_{\tilde{\chi}^0_1} > m_{\tilde{\chi}^0_3}$). The gray area is excluded by $m_{\tilde{\chi}^\pm_1} < 104\,\mathrm{GeV}$

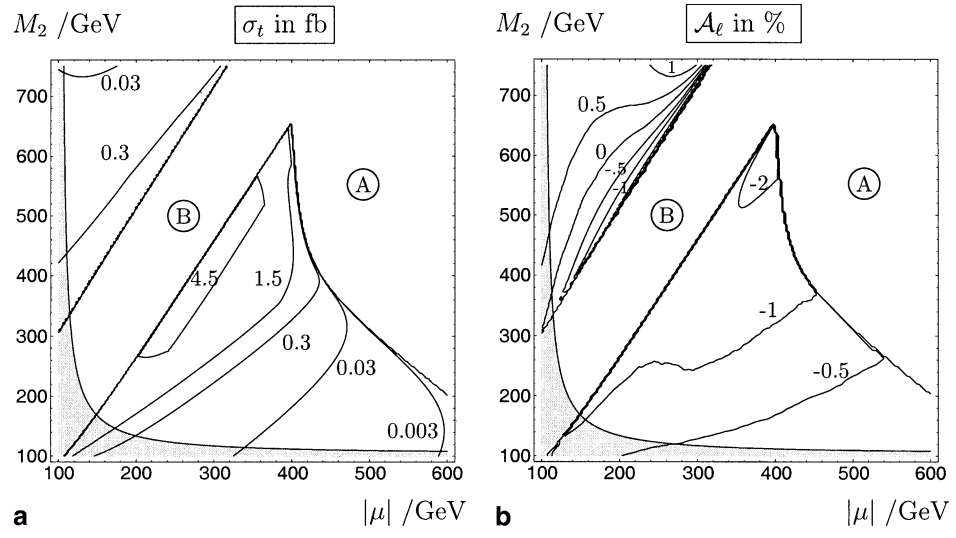

Fig. 8. Contour lines of $\sigma_t = \sigma(e^+e^- \to \tilde{\chi}^0_2\tilde{\chi}^0_3) \times \mathrm{BR}(\tilde{\chi}^0_3 \to Z\tilde{\chi}^0_1) \times \mathrm{BR}(Z \to \ell\bar{\ell})$ **a**, and the asymmetry $\mathcal{A}_\ell$ **b** in the $|\mu|$–M_2 plane for $\varphi_{M_1} = 0.5\pi$, $\varphi_\mu = 0$, taking $\tan\beta = 10$, $m_0 = 300\,\mathrm{GeV}$, $\sqrt{s} = 800\,\mathrm{GeV}$ and $(P_{e^-}, P_{e^+}) = (0.8, -0.6)$. The area A (B) is kinematically forbidden by $m_{\tilde{\chi}^0_2} + m_{\tilde{\chi}^0_3} > \sqrt{s}$ ($m_Z + m_{\tilde{\chi}^0_1} > m_{\tilde{\chi}^0_3}$). The gray area is excluded by $m_{\tilde{\chi}^\pm_1} < 104\,\mathrm{GeV}$

4.4 Production of $\tilde{\chi}^0_2\,\tilde{\chi}^0_3$

For the process $e^+e^- \to \tilde{\chi}^0_2\tilde{\chi}^0_3$ we discuss the decay $\tilde{\chi}^0_3 \to Z\tilde{\chi}^0_1$ of the heavier neutralino which has a larger kinematically allowed region than that of $\tilde{\chi}^0_2 \to Z\tilde{\chi}^0_1$. Similar to $\tilde{\chi}^0_1\,\tilde{\chi}^0_3$ production and decay, the cross section $\sigma(e^+e^- \to \tilde{\chi}^0_2\tilde{\chi}^0_3)$ reaches values up to 50 fb for a beam polarization of $(P_{e^-}, P_{e^+}) = (0.8, -0.6)$. The cross section for the complete process $\sigma_t = \sigma(e^+e^- \to \tilde{\chi}^0_2\tilde{\chi}^0_3) \times \mathrm{BR}(\tilde{\chi}^0_3 \to Z\tilde{\chi}^0_1) \times \mathrm{BR}(Z \to \ell\bar{\ell})$ attains values up to 5 fb in the $|\mu|$–M_2 plane; see Fig. 8a.

The asymmetry $\mathcal{A}_\ell$, Fig. 8b, is somewhat larger than the asymmetry for $\tilde{\chi}^0_1\,\tilde{\chi}^0_3$ production and decay and reaches a maximum of 2%. Although in the respective region the cross section is also a bit larger, $\sigma_t \lesssim 4\,\mathrm{fb}$, it will be difficult to measure $\mathcal{A}_\ell$. For example taking $|\mu| = 380\,\mathrm{GeV}$, $M_2 = 560\,\mathrm{GeV}$ and $(\varphi_{M_1}, \varphi_\mu) = (0.5\pi, 0)$, we have $S_\ell \approx 1$, for $\mathcal{L} = 500\,\mathrm{fb}^{-1}$. However for the hadronic decays of the Z we have $S_{b(c)} \approx 8(5)$ and thus $\mathcal{A}_{b(c)}$ could be measured for $\tilde{\chi}^0_1\,\tilde{\chi}^0_3$ production. Concerning the φ_μ dependence of $\mathcal{A}_\ell$ we found that $|\mathcal{A}_\ell| \lesssim 1\%$ in regions of the $|\mu|$–M_2 plane where $\sigma_t \lesssim 0.5\,\mathrm{fb}$, and $|\mathcal{A}_\ell| \lesssim 0.4\%$ in regions where $\sigma_t \lesssim 5\,\mathrm{fb}$, for example for $\varphi_\mu = 0.5\pi$ and $\varphi_{M_1} = 0$.

5 Summary and conclusions

We have proposed and analyzed CP-sensitive observables in neutralino production $e^+e^- \to \tilde{\chi}^0_i\tilde{\chi}^0_j$ and the subsequent two-body decay of one neutralino into the Z boson $\tilde{\chi}^0_i \to \chi^0_n Z$, followed by the decay $Z \to \ell\bar{\ell}$ for $\ell = e, \mu, \tau$, or $Z \to q\bar{q}$ for $q = c, b$. The CP-sensitive observables are defined by the vector component V_2 of the Z boson density matrix and the CP-asymmetry $\mathcal{A}_{\ell(q)}$, which involves the triple product $\mathcal{T}_{\ell(q)} = \mathbf{p}_{e^-} \cdot (\mathbf{p}_{\ell(q)} \times \mathbf{p}_{\bar{\ell}(\bar{q})})$. The tree-level contributions to these observables are due to correlations of the neutralino $\tilde{\chi}^0_i$ spin and the Z boson spin. In a numerical study of the MSSM parameter space with complex M_1 and μ for $\tilde{\chi}^0_1\tilde{\chi}^0_2$, $\tilde{\chi}^0_2\tilde{\chi}^0_2$, $\tilde{\chi}^0_1\tilde{\chi}^0_3$ and $\tilde{\chi}^0_2\tilde{\chi}^0_3$ production, we have shown that the asymmetry $\mathcal{A}_\ell$ can go up to 3%. For the hadronic decays of the Z boson, larger asymmetries are obtained with $\mathcal{A}_{c(b)} \simeq 6.3(4.5) \times \mathcal{A}_\ell$. By analyzing their statistical errors, we found that the asymmetries $\mathcal{A}_{c(b)}$ could be accessible in future electron positron linear collider experiments in the 500–800 GeV range with high luminosity and longitudinally polarized beams.

Acknowledgements. We thank S. Hesselbach and T. Kernreiter for useful discussions. This work was supported by the "Fonds zur Förderung der wissenschaftlichen Forschung" (FWF) of Austria, projects No. P13139-PHY and No. P16592-N02, by the European Community's Human Potential Programme under contract HPRN-CT-2000-00149 and HPRN-CT-2000-00148 and by Spanish grants BFM2002-00345. This work was also supported by the "Deutsche Forschungsgemeinschaft" (DFG) under contract Fr 1064/5-1. OK was supported by the EU Research Training Site contract HPMT-2000-00124.

A Coordinate frame and spin vectors

We choose a coordinate frame in the laboratory system such that the momentum of the neutralino $\tilde{\chi}_j^0$ points in the z-direction (in our definitions we follow closely [3]). The scattering angle is $\theta = \angle(\mathbf{p}_{e^-}, \mathbf{p}_{\chi_j})$ and the azimuth ϕ can be chosen zero. The momenta are given by

$$\begin{aligned} p_{e^-} &= E_b(1, -\sin\theta, 0, \cos\theta), \\ p_{e^+} &= E_b(1, \sin\theta, 0, -\cos\theta), \end{aligned} \tag{A.1}$$

$$p_{\chi_i} = (E_{\chi_i}, 0, 0, -q), \quad p_{\chi_j} = (E_{\chi_j}, 0, 0, q), \tag{A.2}$$

with the beam energy $E_b = \sqrt{s}/2$ and

$$E_{\chi_i} = \frac{s + m_{\chi_i}^2 - m_{\chi_j}^2}{2\sqrt{s}}, \quad E_{\chi_j} = \frac{s + m_{\chi_j}^2 - m_{\chi_i}^2}{2\sqrt{s}},$$

$$q = \frac{\lambda^{\frac{1}{2}}\left(s, m_{\chi_i}^2, m_{\chi_j}^2\right)}{2\sqrt{s}}, \tag{A.3}$$

where m_{χ_i}, m_{χ_j} are the masses of the neutralinos and $\lambda(x,y,z) = x^2 + y^2 + z^2 - 2(xy + xz + yz)$. We choose the three spin vectors $s_{\chi_i}^{a,\mu}$ $(a = 1,2,3)$ of the neutralino in the laboratory system by

$$\begin{aligned} s_{\chi_i}^1 &= (0, -1, 0, 0), \quad s_{\chi_i}^2 = (0, 0, 1, 0), \\ s_{\chi_i}^3 &= \frac{1}{m_{\chi_i}}(q, 0, 0, -E_{\chi_i}). \end{aligned} \tag{A.4}$$

Together with $p_{\chi_i}^\mu/m_{\chi_i}$ they form an orthonormal set. For the two-body decay $\tilde{\chi}_i^0 \to \tilde{\chi}_n^0 Z$ the decay angle $\theta_1 = \angle(\mathbf{p}_{\chi_i}, \mathbf{p}_Z)$ is constrained by $\sin\theta_1^{\max} = q^0/q$ for $q > q^0$, where $q^0 = \lambda^{\frac{1}{2}}(m_{\chi_i}^2, m_Z^2, m_{\chi_n}^2)/2m_Z$ is the neutralino momentum if the Z boson is produced at rest. In this case there are two solutions:

$$\begin{aligned} |\mathbf{p}_Z^\pm| = \Big\{ &\left(m_{\chi_i}^2 + m_Z^2 - m_{\chi_n}^2\right) q\cos\theta_1 \\ &\pm E_{\chi_i}\left[\lambda\left(m_{\chi_i}^2, m_Z^2, m_{\chi_n}^2\right) - 4q^2 m_Z^2\left(1 - \cos^2\theta_1\right)\right]^{\frac{1}{2}} \Big\} \\ / &\left\{2q^2\left(1 - \cos^2\theta_1\right) + 2m_{\chi_i}^2\right\}. \end{aligned} \tag{A.5}$$

If $q^0 > q$, θ_1 is not constrained and there is only the physical solution $|\mathbf{p}_Z^+|$ left. The momenta in the laboratory system are

$$p_Z^\pm = \left(E_Z^\pm, -|\mathbf{p}_Z^\pm|\sin\theta_1\cos\phi_1, |\mathbf{p}_Z^\pm|\sin\theta_1\sin\phi_1, -|\mathbf{p}_Z^\pm|\cos\theta_1\right), \tag{A.6}$$

$$p_{\bar{f}} = \left(E_{\bar{f}}, -|\mathbf{p}_{\bar{f}}|\sin\theta_2\cos\phi_2, |\mathbf{p}_{\bar{f}}|\sin\theta_2\sin\phi_2, -|\mathbf{p}_{\bar{f}}|\cos\theta_2\right), \tag{A.7}$$

$$E_{\bar{f}} = |\mathbf{p}_{\bar{f}}| = \frac{m_Z^2}{2\left(E_Z^\pm - |\mathbf{p}_Z^\pm|\cos\theta_{D_2}\right)}, \tag{A.8}$$

with $\theta_2 = \angle(\mathbf{p}_{\chi_i}, \mathbf{p}_{\bar{f}})$ and the decay angle $\theta_{D_2} = \angle(\mathbf{p}_Z, \mathbf{p}_{\bar{f}})$ given by

$$\cos\theta_{D_2} = \cos\theta_1\cos\theta_2 + \sin\theta_1\sin\theta_2\cos(\phi_2 - \phi_1). \tag{A.9}$$

The spin vectors $t_Z^{c,\mu}$ $(c = 1,2,3)$ of the Z boson in the laboratory system are chosen by

$$\begin{aligned} t_Z^1 &= \left(0, \frac{\mathbf{t}_Z^2 \times \mathbf{t}_Z^3}{|\mathbf{t}_Z^2 \times \mathbf{t}_Z^3|}\right), \quad t_Z^2 = \left(0, \frac{\mathbf{p}_{e^-} \times \mathbf{p}_Z}{|\mathbf{p}_{e^-} \times \mathbf{p}_Z|}\right), \\ t_Z^3 &= \frac{1}{m_Z}\left(|\mathbf{p}_Z|, E_Z\frac{\mathbf{p}_Z}{|\mathbf{p}_Z|}\right). \end{aligned} \tag{A.10}$$

The spin vectors and p_Z^μ/m_Z form an orthonormal set. The polarization vectors $\varepsilon^{\lambda_k,\mu}$ for helicities $\lambda_k = -1, 0, +1$ of the Z boson are defined by

$$\begin{aligned} \varepsilon^- &= \tfrac{1}{\sqrt{2}}\left(t_Z^1 - \mathrm{i}t_Z^2\right); \\ \varepsilon^0 &= t_Z^3; \\ \varepsilon^+ &= -\tfrac{1}{\sqrt{2}}\left(t_Z^1 + \mathrm{i}t_Z^2\right). \end{aligned} \tag{A.11}$$

B Phase space

The Lorentz invariant phase space element for the neutralino production (6) and the decay chain (7) and (8) can be decomposed into the two-body phase space elements:

$$\begin{aligned} &\mathrm{dLips}\left(s, p_{\chi_j}, p_{\chi_n}, p_f, p_{\bar{f}}\right) \\ &= \frac{1}{(2\pi)^2}\,\mathrm{dLips}\left(s, p_{\chi_i}, p_{\chi_j}\right) \\ &\quad \times \mathrm{d}s_{\chi_i}\sum_\pm \mathrm{dLips}\left(s_{\chi_i}, p_{\chi_n}, p_Z^\pm\right)\,\mathrm{d}s_Z\mathrm{dLips}\left(s_Z, p_f, p_{\bar{f}}\right), \end{aligned} \tag{B.1}$$

$$\mathrm{dLips}\left(s, p_{\chi_i}, p_{\chi_j}\right) = \frac{q}{8\pi\sqrt{s}}\,\sin\theta\,\mathrm{d}\theta, \tag{B.2}$$

$$\begin{aligned} &\mathrm{dLips}\left(s_{\chi_i}, p_{\chi_n}, p_Z^\pm\right) \\ &= \frac{1}{2(2\pi)^2}\,\frac{|\mathbf{p}_Z^\pm|^2}{2|E_Z^\pm\, q\cos\theta_1 - E_{\chi_i}\,|\mathbf{p}_Z^\pm||}\,\mathrm{d}\Omega_1, \end{aligned} \tag{B.3}$$

$$\mathrm{dLips}\left(s_Z, p_f, p_{\bar{f}}\right) = \frac{1}{2(2\pi)^2}\,\frac{|\mathbf{p}_{\bar{f}}|^2}{m_Z^2}\,\mathrm{d}\Omega_2, \tag{B.4}$$

with $s_{\chi_i} = p_{\chi_i}^2$, $s_Z = p_Z^2$ and $\mathrm{d}\Omega_i = \sin\theta_i\,\mathrm{d}\theta_i\,\mathrm{d}\phi_i$. We use the narrow width approximation for the propagators: $\int|\Delta\left(\tilde{\chi}_i^0\right)|^2\mathrm{d}s_{\chi_i} = \frac{\pi}{m_{\chi_i}\Gamma_{\chi_i}}$, $\int|\Delta(Z)|^2\mathrm{d}s_Z = \frac{\pi}{m_Z\Gamma_Z}$. The approximation is justified for $(\Gamma_{\chi_i}/m_{\chi_i})^2 \ll 1$, which holds in our case with $\Gamma_{\chi_i} \lesssim \mathcal{O}(1\,\mathrm{GeV})$.

C Spin matrices

In the basis (A.11) the spin matrices J^c and the tensor components J^{cd} are

$$J^1 = \begin{pmatrix} 0 & \frac{1}{\sqrt{2}} & 0 \\ \frac{1}{\sqrt{2}} & 0 & \frac{1}{\sqrt{2}} \\ 0 & \frac{1}{\sqrt{2}} & 0 \end{pmatrix}, \quad J^2 = \begin{pmatrix} 0 & \frac{\mathrm{i}}{\sqrt{2}} & 0 \\ -\frac{\mathrm{i}}{\sqrt{2}} & 0 & \frac{\mathrm{i}}{\sqrt{2}} \\ 0 & -\frac{\mathrm{i}}{\sqrt{2}} & 0 \end{pmatrix},$$

$$J^3 = \begin{pmatrix} -1 & 0 & 0 \\ 0 & 0 & 0 \\ 0 & 0 & 1 \end{pmatrix}, \tag{C.1}$$

$$J^{11} = \begin{pmatrix} -\frac{1}{3} & 0 & 1 \\ 0 & \frac{2}{3} & 0 \\ 1 & 0 & -\frac{1}{3} \end{pmatrix}, \quad J^{22} = \begin{pmatrix} -\frac{1}{3} & 0 & -1 \\ 0 & \frac{2}{3} & 0 \\ -1 & 0 & -\frac{1}{3} \end{pmatrix},$$

$$J^{33} = \begin{pmatrix} \frac{2}{3} & 0 & 0 \\ 0 & -\frac{4}{3} & 0 \\ 0 & 0 & \frac{2}{3} \end{pmatrix}, \tag{C.2}$$

$$J^{12} = \begin{pmatrix} 0 & 0 & \mathrm{i} \\ 0 & 0 & 0 \\ -\mathrm{i} & 0 & 0 \end{pmatrix}, \quad J^{23} = \begin{pmatrix} 0 & -\frac{\mathrm{i}}{\sqrt{2}} & 0 \\ \frac{\mathrm{i}}{\sqrt{2}} & 0 & \frac{\mathrm{i}}{\sqrt{2}} \\ 0 & -\frac{\mathrm{i}}{\sqrt{2}} & 0 \end{pmatrix},$$

$$J^{13} = \begin{pmatrix} 0 & -\frac{1}{\sqrt{2}} & 0 \\ -\frac{1}{\sqrt{2}} & 0 & \frac{1}{\sqrt{2}} \\ 0 & \frac{1}{\sqrt{2}} & 0 \end{pmatrix}. \tag{C.3}$$

References

1. H.E. Haber, G.L. Kane, Phys. Rept. **117**, 75 (1985)
2. S.Y. Choi, J. Kalinowski, G. Moortgat-Pick, P.M. Zerwas, Eur. Phys. J. C **22**, 563 (2001) [Addendum C **23**, 769 (2002)] [hep-ph/0108117]
3. G. Moortgat-Pick, H. Fraas, A. Bartl, W. Majerotto, Eur. Phys. J. C **9**, 521 (1999) [Erratum C **9**, 549 (1999)] [hep-ph/9903220]
4. Y. Kizukuri, N. Oshimo, Phys. Lett. B **249**, 449 (1990)
5. S.Y. Choi, H.S. Song, W.Y. Song, Phys. Rev. D **61**, 075004 (2000) [hep-ph/9907474]
6. J.F. Donoghue, Phys. Rev. D **18**, 1632 (1978); G. Valencia, hep-ph/9411441
7. A. Bartl, H. Fraas, O. Kittel, W. Majerotto, Phys. Rev. D **69**, 035007 (2004) [hep-ph/0308141]; A. Bartl, H. Fraas, O. Kittel, W. Majerotto, hep-ph/0308143
8. A. Bartl, T. Kernreiter, O. Kittel, Phys. Lett. B **578**, 341 (2004) [hep-ph/0309340]; S.Y. Choi, M. Drees, B. Gaissmaier, J. Song, hep-ph/0310284
9. A. Bartl, H. Fraas, T. Kernreiter, O. Kittel, Eur. Phys. J. C **33**, 433 (2004) [hep-ph/0306304]
10. S.Y. Choi, Y.G. Kim, Phys. Rev. D **69**, 015011 (2004) [hep-ph/0311037]
11. H.E. Haber, Proceedings of the 21st SLAC Summer Institute on Particle Physics, edited by L. DeProcel, Ch. Dunwoodie, Stanford 1993, 231
12. S.Y. Choi, T. Lee, H.S. Song, Phys. Rev. D **40**, 2477 (1989); H.S. Song, Phys. Rev. D **33**, 1252 (1986), A. Bacchetta, P.J. Mulders, Phys. Rev. D **62**, 114004 (2000) [hep-ph/0007120]
13. C.J. Damerell, D.J. Jackson, Prepared for 1996 DPF / DPB Summer Study on New Directions for High-Energy Physics (Snowmass 96), Snowmass, Colorado, 25 June–12 July 1996; K. Abe et al. [SLD Collaboration], Phys. Rev. Lett. **88**, 151801 (2002); S.M. Xella-Hansen, M. Wing, D.J. Jackson, N. de Groot, C.J.S. Damerell, Update on flavour tagging studies for the Future Linear Collider using the Brahms simulation, LC-PHSM-2003-061
14. B. Aubert et al. [BABAR Collaboration], Phys. Rev. D **66**, 032003 (2002)
15. K. Hagiwara et al. [Particle Data Group Collaboration], Phys. Rev. D **66**, 010001 (2002)
16. L.J. Hall, J. Polchinski, Phys. Lett. B **152**, 335 (1985)
17. W. Oller, H. Eberl, W. Majerotto, hep-ph/0402134
18. See, e.g., A. Bartl, T. Gajdosik, W. Porod, P. Stockinger, H. Stremnitzer, Phys. Rev. D **60**, 073003 (1999) [hep-ph/9903402]; A. Bartl, T. Gajdosik, E. Lunghi, A. Masiero, W. Porod, H. Stremnitzer, O. Vives, Phys. Rev. D **64**, 076009 (2001) [hep-ph/0103324]; for a review see T. Ibrahim, P. Nath, hep-ph/0107325
19. A. Bartl, W. Majerotto, W. Porod, D. Wyler, Phys. Rev. D **68**, 053005 (2003) [hep-ph/0306050]